The American Journal of Pathology, Vol. 175, No. 6, December 2009

DOI: 10.2353/ajpath.2009.080930

Cardiovascular, Pulmonary and Renal Pathology

Dysferlin Deficiency and the Development of Cardiomyopathy in a Mouse Model of Limb-Girdle Muscular Dystrophy 2B

Thomas H. Chase, Gregory A. Cox, Lisa Burzenski, Oded Foreman, and Leonard D. Shultz

From The Jackson Laboratory, Bar Harbor, Maine

Limb-girdle muscular dystrophy 2B, Miyoshi myopathy, and distal myopathy of anterior tibialis are severely debilitating muscular dystrophies caused by genetically determined dysferlin deficiency. In these muscular dystrophies, it is the repair, not the structure, of the plasma membrane that is impaired. Though much is known about the effects of dysferlin deficiency in skeletal muscle, little is known about the role of dysferlin in maintenance of cardiomyocytes. Recent evidence suggests that dysferlin deficiency affects cardiac muscle, leading to cardiomyopathy when stressed. However, neither the morphological location of dysferlin in the cardiomyocyte nor the progression of the disease with age are known. In this study, we examined a mouse model of dysferlinopathy using light and electron microscopy as well as echocardiography and conscious electrocardiography. We determined that dysferlin is normally localized to the intercalated disk and sarcoplasm of the cardiomyocytes. In the absence of dysferlin, cardiomyocyte membrane damage occurs and is localized to the intercalated disk and sarcoplasm. This damage results in transient functional deficits at 10 months of age, but, unlike in skeletal muscle, the cell injury is sublethal and causes only mild cardiomyopathy even at advanced ages. ***(Am J Pathol 2009, 175:2299–2308; DOI: 10.2353/ajpath.2009.080930)***

Plasma membrane damage in mechanically active cells such as the myocyte is inevitable even under normal physiological conditions.[1,2] Since membranes are not self-sealing, effective and efficient repair mechanisms are necessary to maintain cell viability. Dysferlin plays a central role in this active repair mechanism in skeletal muscle. In the absence of dysferlin disruptions of the skeletal muscle plasma membrane are not repaired leading to cell death.[3] Skeletal muscle can regenerate new cells from satellite cells but eventually even this response is exhausted, and lost myocytes are replaced by fat and fibrosis resulting in debilitating muscular dystrophy.

Limb-girdle muscular dystrophy type 2 B (LGMD2B), Miyoshi myopathy, and distal myopathy of anterior tibialis are three clinically distinct forms of muscular dystrophy that are caused by mutations within the dysferlin (*DYSF*) gene resulting in severe to complete deficiency of dysferlin expression.[4,5] Clinically, these dysferlinopathies start in young adulthood with progressive muscle weakness and atrophy that advances to severe disability in older adulthood.

Dysferlin is a 273 kDa membrane-spanning protein with multiple C2 domains that bind calcium, phospholipids, and proteins to then trigger signaling events, vesicle trafficking, and membrane fusion.[6,7] The name "dysferlin" reflects the homology with FER-1, the *Caenorhabditis elegans* spermatogenesis factor involved in the fusion of vesicles with the plasma membrane, as well as the dystrophic phenotype associated with its deficiency.[5] Dysferlin is crucial to calcium dependent membrane repair in muscle cells.[3,8] In normal skeletal muscle, sarcolemma injuries lead to the accumulation of dysferlin-enriched membrane patches and resealing of the membrane in the presence of Ca^{2+}.[3,9]

While the profound effect of dysferlin deficiency in skeletal muscle has been the subject of much investigation, the effect of dysferlin deficiency in cardiac muscle has largely been ignored. However, in 2004, Kuru et al[10] reported on a 57-year-old Japanese woman with LGMD2B and dilated cardiomyopathy; more recently, Wenzel et al[11] described dilated cardiomyopathy in two

Supported by the Ruth L. Kirschstein National Research Service Award, (T 32), RR-070 68-07TC, National Institutes of Health grant HL077642, and National Institutes of Health Cancer Core grant CA 34196.

Accepted for publication August 13, 2009.

Supplemental material for this article can be found on *http://ajp.amjpathol.org.*

Address reprint requests to Leonard D. Shultz, The Jackson Laboratory, 600 Main St, Bar Harbor, ME 04609. E-mail: lenny.shultz@jax.org.

out of seven patients with LGMD2B and other cardiac abnormalities in three of the others. These observations suggest that dysferlin deficiency can lead to cardiomyopathy as well as to muscular dystrophy. However, neither the morphological location of dysferlin in the cardiomyocyte nor the progression of the disease with age are known.

Spontaneous mutations in the mouse are valuable resources in understanding human disease processes. Genetically defined mice develop dysferlinopathies closely resembling LGMD2B, Miyoshi myopathy, and distal myopathy of anterior tibialis.[12] In 2004, Ho et al[12] identified A/J mice as dysferlin deficient. A retrotransposon insertion in the dysferlin gene was found to result in a null allele, resulting in skeletal muscle dystrophy that shows histopathological and ultrastructural features that closely resemble the human dysferlinopathies of LGMD2B, Miyoshi myopathy, and distal myopathy of anterior tibialis.[12] The onset of dystrophic features in A/J mice begins in proximal limb muscles at 4 to 5 months of age and progresses to severe debilitating muscular dystrophy over several months. Ho et al[12] also found that human and murine dysferlin share very similar (approximately 90% identity) amino acid sequences. Cardiac muscle was not included in their study.

Recently, Han et al,[8] using sucrose gradient membrane fractionation on homogenates of wild-type C57BL/6J mouse heart muscle, showed that dysferlin is present in the cardiomyocyte plasma membrane and intracellular vesicle fractions. It was proposed that dysferlin is localized to the cardiomyocyte sarcolemma and some unidentified type of vesicles.[8] Han et al[8] in one study and Wenzel et al[11] in another study showed that the induction of significant cardiac stress lead to cardiac dysfunction in dysferlin-deficient mice, but to what extent dysferlin deficiency causes cardiomyopathy by aging alone in patients clinically affected with the debilitating effects of LGMD2B, Miyoshi myopathy, or distal myopathy of anterior tibialis is unknown.

In this study, we used the A/J mouse model to study the effects of aging in mice affected by genetically determined dysferlin deficiency by using echocardiography and conscious electrocardiography to determine functional changes *in vivo*, followed postmortem by light and electron microscopy to determine associated morphological changes. We have determined that the normal primary location for dysferlin in the cardiomyocyte of control A/HeJ mice is the intercalated disk (ID), and to a lesser extent, to a distinctive transverse banding pattern within the sarcoplasm of the cardiomyocyte. We have also determined that in the dysferlin-deficient cardiomyocyte there is evidence of membrane damage at these locations. We also present data that show functional cardiac deficits were present *in vivo* at around 10 months of age then recovered by 12 months. Histopathology showed that under normal laboratory conditions dysferlin deficiency causes only a mild cardiomyopathy even at advanced ages, suggesting the possibility of dysferlin-independent membrane repair mechanisms in cardiac muscle that do not exist in skeletal muscle.

Materials and Methods

Animals

Both A/J and the substrain A/HeJ mice were obtained from the Jackson Laboratory (Bar Harbor, ME). All animals were bred, housed, and maintained in a barrier facility at the Jackson Laboratory under standard conditions with a 12-hour light to 12-hour dark cycle and were provided food (Purina LabDiet Richmond, Indiana; 6%, autoclaved) and water *ad libitum*. The experimental protocols were approved by the Jackson Laboratory Institutional Animal Care and Use Committee, and are in accordance with accepted institutional and governmental policies.

Histology

All mice in this study were subjected to necropsy and histopathology. For routine histopathology and immunohistochemical studies cardiac and skeletal muscle tissues as well as other tissues were harvested and fixed in Tellyesniczky/Fekete fixative. Most hearts were sectioned in either the four chamber longitudinal cut or transversely at the equator, base, and apex. For animals to be examined by electron microscopy as well as light microscopy, perfusion with 2% gluteraldehyde, 2% paraformaldehyde, and 0.5% tannic acid was followed by fixation in Tellyesniczky/Fekete fixative overnight. Tissues were then dehydrated and paraffin embedded for routine H&E and Masson's Trichrome staining.

Morphometric Assessment of Myocardial Condition

The morphometric index most frequently assessed is myocardial fibrosis.[13] Both semiquantitative and quantitative methods were used as described[13,14] to report the condition of the myocardium.

Briefly, digital photographs of the myocardium were taken at 400× magnification on an Olympus CX41 (Olympus, Center Valley, PA) microscope equipped with a Leica DX320 (Lelca, Solms, Germany) color camera using Leica software. Color-subtractive computer-assisted image analysis in Image J software (NIH freeware, *http://rsbweb.nih.gov.ij/*) was used to quantify the percentage of collagen as described.[14] Additionally, tissues sections were examined by a board certified veterinary pathologist specializing in murine pathology (O.F.). A semiquantitative method was used as described[13] in the assessment of the condition of the myocardium and scored as follows: 0 = normal; 1 = mild degenerative changes, including vacuolation; 2 = moderate degenerative changes, including widespread vacuolation with increased fibrosis; and 3 = severe changes including necrosis, large areas of interstitial fibrosis, and significant loss of cardiomyocytes. The incidental occurrence of the epicardial fibrosis/calcification lesion that is common in A/J and other strains of mice was excluded from consideration in this study.

Immunohistochemistry

Slides of paraffin embedded sections were deparaffinized and rehydrated. Endogenous peroxidase activity was blocked with 3% hydrogen peroxide. Retrievagen A (BD Biosciences, San Diego, CA) was used per directions for antigen retrieval. Antigens were denatured with 100 mmol/L glycine in PBS then 0.05% SDS in PBS for 30 minutes at 50°C. Primary antibodies were mouse monoclonal anti-dysferlin (Clone Ham1/7B6) (Lab Vision/NeoMarkers; Fremont, CA) and rabbit polyclonal to Connexin 43/GJA1 (Abcam; Cambridge, MA). To control for nonspecific staining mouse on mouse (MOM) (PK-2200; Vector Laboratories; Burlingame, CA) diluent alone was applied to control sections. Nonspecific secondary binding was blocked and sections were developed by using the peroxidase MOM kit (PK-2200; Vector Laboratories) per directions, then counterstained with Meyer's Hematoxalin.

Transmission Electron Microscopy

Mice necropsied for transmission electron microscopy (TEM) were perfused with 2% gluteraldehyde, 2% paraformaldehyde, and 0.5% tannic acid in 0.1 M cacodylate buffer, pH 7.4. Tissues for TEM were harvested from the left ventricle, right ventricle, and the interventricular septum, then submerged in EM fix, minced, fixed overnight, then postfixed with 1% osmium tetroxide (0.1 M cacodylate buffer, pH 7.4). The samples were then rinsed in the same buffer, dehydrated in a graded series of ethanols, and embedded in Epon Araldite resin (Electron Microscopy Sciences; Hatfield, PA). Ultrathin sections were poststained with uranyl acetate followed by lead citrate. Samples were imaged on a JEOL JEM-1230 electron microscope (Tokyo, Japan) and images were captured with AMT Advantage CCD 6 Mpix (Danvers, MA) and Image Capture Engine Software version 54.4.2.236.

Assessment of Cardiac Function

In this longitudinal assessment of cardiovascular function, echocardiography and conscious electrocardiograms were done on groups of control (A/HeJ) and dysferlin-deficient (A/J) mice at 3, 5, 8, 9, 10, 12, 14, and 16 to 18 months of age both male and female. No sex differences were seen. Cardiac electrical activity was recorded from conscious mice gently restrained in a Murine ECG Restrainer plexiglas cylinder (QRS Phenotyping, Inc; Calgary, Canada) by using gel-foot pads (EMPI; St Paul, MN) to collect the signal. Signal acquisition was obtained by a PowerLab ARV module version 5.5.4 and ECG analysis module for chart version 2 (AD Instruments; Golden, CO). Mice were allowed to acclimate for 5 to 10 minutes after which the ECG signal was recorded for up to 5 minutes or until a steady baseline lead I signal was recorded for a 20 to 30 second interval. All of the standard P, QRS, and T wave intervals and amplitudes were measured and the signal was averaged as described.[15]

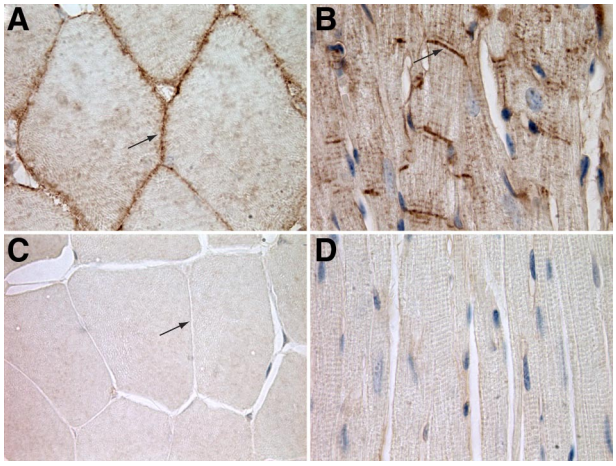

Figure 1. A: In control, dysferlin-sufficient A/HeJ mice skeletal muscle dysferlin is localized to lateral sarcolemma (**arrow**) (HRP anti-dysferlin antibody). **B:** In cardiac muscle of these same control mice, dysferlin is localized primarily to the ID (**arrow**). There is also a transverse striated pattern in the sarcoplasm (HRP anti-dysferlin antibody). **C:** Cross section of A/J skeletal muscle stained for dysferlin, showing the lack of staining of the lateral sarcolemma (HRP anti-dysferlin antibody) (**arrow**). **D:** Longitudinal section of A/J cardiac muscle stained for dysferlin, demonstrating a lack of dysferlin staining (HRP anti-dysferlin antibody). Original magnification, ×1000.

Following the conscious electrocardiograms, echocardiography was performed on the same groups of A/J and A/HeJ mice at these ages from 3 to 18 months. The Vevo 770 High-Frequency Ultrasound (Visualsonics; Toronto, Ontario, Canada) was used to obtain real-time images of cardiac function. A 30 MHz real-time microvisualization scan head yielded ultrasonic images with an infiltration depth of 13 mm, and a capture rate of 100 Hz. Animals were induced individually with 5% isoflurane at 0.8 L/min and maintained on 1 to 1.5% isoflurane at 0.8 L/min. Hair was removed from the ventral thorax with a depilatory cream, just before standard imaging, measurements, and calculations were performed as described.[15]

Statistics

All values are presented as means ± SEM. Student's paired *t*-test was applied to determine statistical significances. P values <0.05 were considered significant. Statistical analyses were performed by using Prism software (Irvine, CA).

Results

In the Normal Cardiomyocyte Dysferlin is Localized to the ID and Sarcoplasm

Tissue sections of skeletal and cardiac muscle from unmanipulated control A/HeJ and dysferlin-deficient A/J mice were stained with anti-dysferlin antibody and horseradish peroxidase (HRP). In agreement with the known localization, dysferlin staining was localized to the sarcolemma in skeletal muscle in control A/HeJ mice (Figure 1A). In control cardiac muscle, longitudinally sectioned cardiomyocytes showed intense staining of the IDs (Figure 1B). Additionally, in the sarcoplasm there was stain-

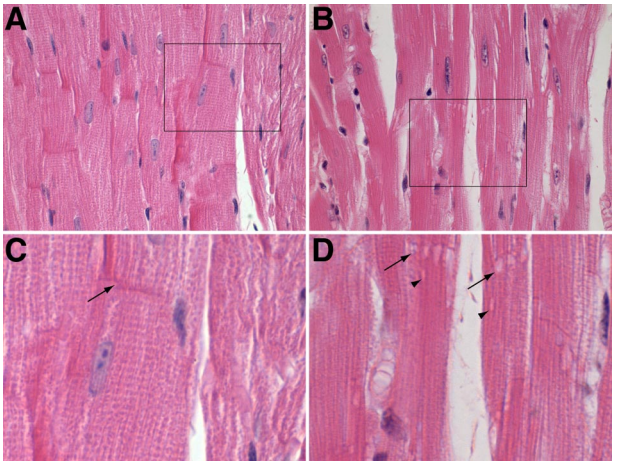

Figure 2. A: Longitudinal sections showing normal myocardium of the control A/HeJ mice had histologically normal myocardium and ID. **B:** Dysferlin-deficient A/J mice develop vacuolations at the ID. **C:** An enlargement of boxed area in **A**, the normal ID can be seen (**arrow**). **D:** An enlargement of boxed area in **B**, here vacuolations can be seen at the ID (**arrow**) and in the sarcoplasm not associated with the ID (**arrowheads**). All are H&E stained. Original magnification: ×600 (**A** and **B**); ×1000 (**C** and **D**).

ing in a transverse striation pattern at regular intervals the length of a sarcomere. Cardiomyocytes oriented in cross section did not show dysferlin staining of the lateral sarcolemma (data not shown). Similar staining patterns were present at various ages and in Balb/cByJ, C57BR/cdJ, and C57BL/6J mice (data not shown). In the dysferlin-deficient A/J mice, staining for dysferlin was negative in both skeletal muscle (Figure 1C) and cardiac muscle (Figure 1D).

Routine Histopathology Shows Evidence of Cell Injury in Cardiomyocytes of Dysferlin-Deficient A/J Mice

Examination of H&E and Masson's trichrome stained hearts of 6-month-old A/HeJ mice showed normal cardiomyocytes (Figure 2A) and ID (arrow Figure 2C), whereas dysferlin-deficient A/J mice showed widespread sarcoplasmic vacuolar degeneration of the majority of cardiomyocytes (Figure 2B), often with multiple vacuolations at the ID of cardiomyocytes (arrow Figure 2B), as well as vacuolations in the sarcoplasm (Figure 2D).

Dysferlin-Deficient Mice Do Not Have Conduction Disturbances of Myocardium

Since vacuolar degeneration is a manifestation of cell injury, usually due to membrane damage, and the ID is a critical structure in the transmission of electrical impulse from one cardiomyocyte to another, membrane damage at this location could disrupt electrical conduction. Therefore, ECGs were done to assess electrical conduction in the myocardium. The following intervals were measured: P duration (intra-atrial conduction); PR interval (intra-atrial and atrio-ventricular conduction); QRS interval (intraventricular conduction); QT interval (ventricular conduction to repolarization of ventricle); and RR interval (length of full cycle). Results of these ECGs indicated that none of these intervals were significantly different in dysferlin-deficient mice compared with controls at all age intervals tested from 5 to 20 months (data not shown). In addition, none of the amplitudes (P, Q, R, S, or T) were significantly different from those of controls (data not shown).

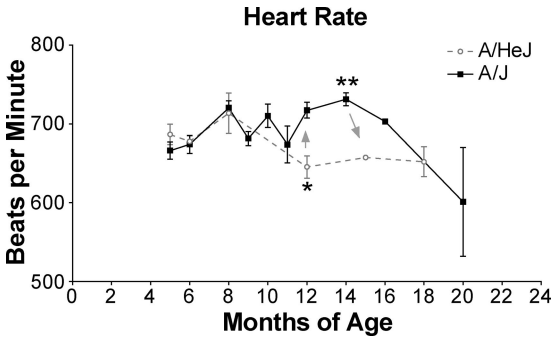

Figure 3. Compared with controls, dysferlin-deficient A/J mice have significantly elevated heart rates from 12 to 18 months of age. This increased rate peaked at 14 months then declined steadily. There were three to eight mice per group; no sex differences were found so males and females were grouped. $*P = .0169$, $**P = .0027$.

The only parameter that was significantly different from the controls was the increased heart rates of 12- to 16-month-old A/J mice. This increased heart rate peaked at 14 months of age before declining thereafter (Figure 3). There are several possible explanations for this increased heart rate (ie, pain and/or declining cardiovascular conditioning due to skeletal muscle disease, or an early sign of compensation for reduced cardiomyocyte contractility) but it is not reflective of a conduction disturbance.

Cardiac Function Declines Temporarily at 10 Months in Unmanipulated Dysferlin-Deficient A/J Mice

High-frequency ultrasound was used to obtain real-time echocardiographic images to evaluate cardiac function. Ejection fraction (EF) and fractional shortening (FS) are echocardiographic indicators of overall cardiac function. EF, a measure of left ventricular function, is the percentage of blood that is pumped out of the ventricle with each beat. EFs above 60% are considered normal.[16] There was no significant difference in EF between control A/HeJ (75 to 77%) and dysferlin-deficient A/J mice (71 to 79%) from 3 months of age to 8 months of age (Figure 4A). After 8 months the EF of A/J mice declined significantly until by 10 months of age it was reduced to 61%, while A/HeJ mice retained a normal EF (82%). By 12 months of age EF for A/J mice rebounded to 75% and remained nearly at that level for the next 8 months. The EF of A/HeJ mice was only slightly higher at 78% during that time.

FS is another measure of left ventricular contractility. It is a ratio of the difference in the diameter of the left ventricle between the contracted and the relaxed states. It has the advantage of being a ratio of actual measurements, whereas ejection fraction is a ratio of three-dimensional quantities derived from two-dimensional measurements. Fractional shortening values greater than 30% are

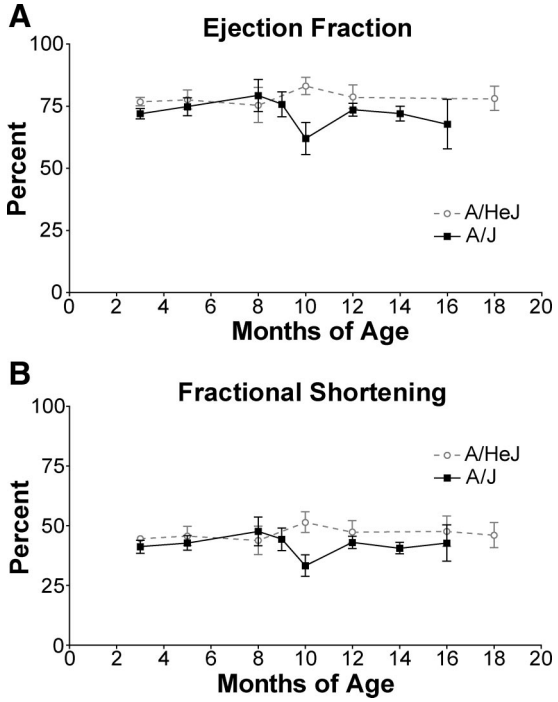

Figure 4. A: There was a significant decrease in EF in dysferlin-deficient A/J mice at 10 months of age followed by recovery at 12 months of age; $*P = 0.0204$. **B:** Similarly, there was a significant decrease in FS in dysferlin-deficient A/J mice at 10 months of age that recovered by 12 months of age. There were 3 to 14 mice per group. Since there were no sex differences, males and females were grouped together.$*P = 0.0193$.

considered normal.[16] As with EF, both A/HeJ and A/J mice had normal FS of 42 to 47% until 8 months of age (Figure 4B). From 8 to 10 months of age the FS of A/J but not A/HeJ decreased to 33%, then rebounded by 12 months of age to 42%. These data suggest that in dysferlin-deficient A/J mice there is a significant deterioration in contractility from 8 to 10 months of age, and a recovery from 10 months of age to 12 months of age. Subsequently, EF and FS of A/J mice remained slightly below that of A/HeJ mice but both continue within the range of normal for the remainder of the study (18 months of age).

Dysferlin-Deficient A/J Mice Show Ultrastructural Evidence of Membrane Disruptions of the IDs

To further assess the nature of the early morphological changes, TEM was done on A/J and A/HeJ mice beginning at 5 months of age. At 5 months of age the ultrastructure of cardiomyocytes, including the ID, was normal in A/HeJ mice (Figure 5A) as well as A/J dysferlin-deficient mice (Figure 5B). In 6-month-old A/HeJ control mice, the IDs were normal (Figure 5C), while in age-matched dysferlin-deficient A/J mice there were occasionally cardiomyocytes that had membrane disruptions and/or delaminations (long arrow Figure 5D) associated with the fascia adherens (FA) portion of the substructure of the ID. Near the ID there were also occaisonal vacuolations (Figure 5E). Some of these vacuolations were dilations of the sarcoplastic reticulum while others were

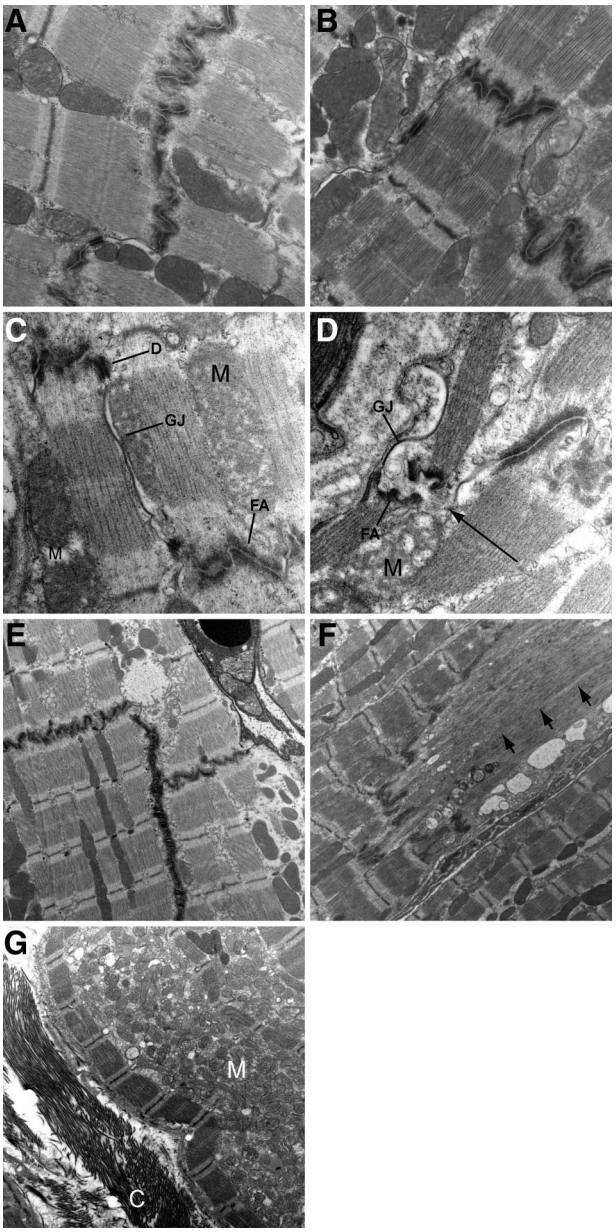

Figure 5. TEM of unmanipulated dysferlin-sufficient A/HeJ and dysferlin-deficient A/J cardiac muscle. At 5 months of age, both A/HeJ (**A**) and A/J mice (**B**) have normal cardiomyocytes and IDs. At 6 months, as compared with the normal A/HeJ ID (**C**) the GJ of the A/J mice (**D**) are distorted but appear to be intact. The FA at the ends of the contractile apparatus have been pulled apart and there is a membrane defect (**arrow**). Occasionally, there are vacuoles present near the ID (**E**). Occasionally, necrotic cardiomyocytes were seen with vacuolations at or near the ID and loss of sarcomeric structure (**arrow, F**). In some older A/J mice, there was a marked reduction in the myofibril density, large accumulations of mitochondria, and extracellular collagen (**G**). C = collagen; D = desmosome; M = mitochondrion; GJ = gap junction and FA = fascia adherens. Original magnification: ×30,000 (**A** and **B**); ×50,000 (**C** and **D**); ×15,000 (**E**); ×12,000 (**F** and **G**).

mitochondria that were swollen to 5 to 10 times normal size with destruction of the cristae (high amplitude swelling). TEM also showed that there were similar vacuolations between myofibrils unassociated with the ID. The desmosomes were normal, and most gap junctions (GJ) of dysferlin-deficient A/J mice were normal but occasionally there were GJ that appeared distorted yet intact (GJ

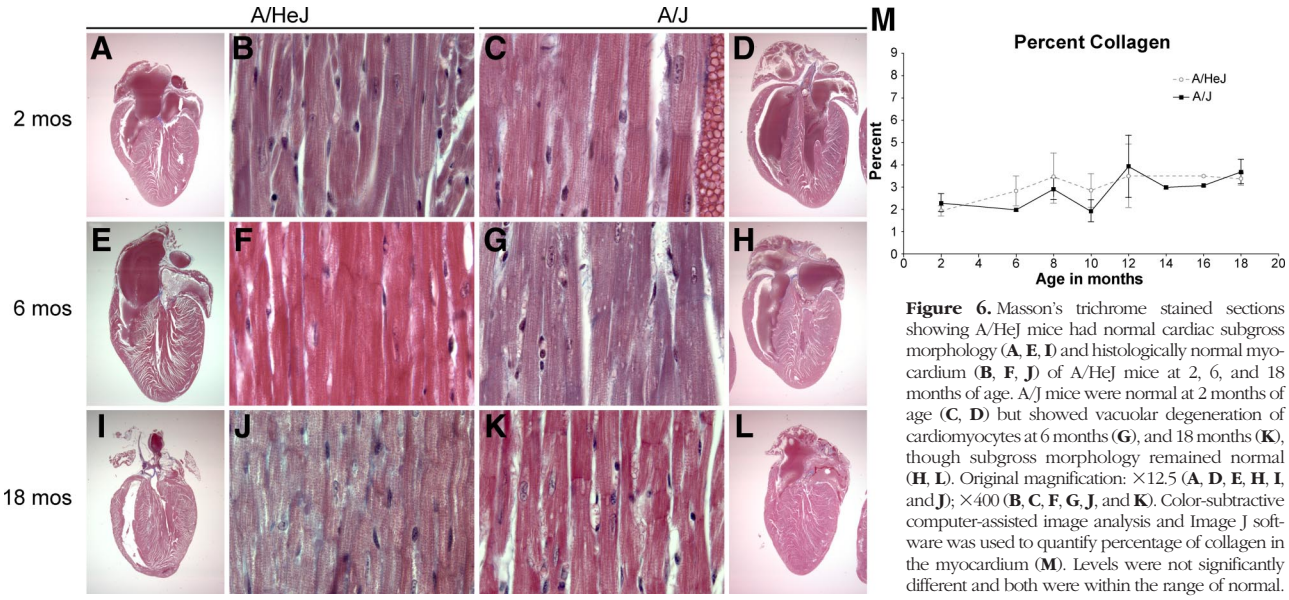

Figure 6. Masson's trichrome stained sections showing A/HeJ mice had normal cardiac subgross morphology (**A**, **E**, **I**) and histologically normal myocardium (**B**, **F**, **J**) of A/HeJ mice at 2, 6, and 18 months of age. A/J mice were normal at 2 months of age (**C**, **D**) but showed vacuolar degeneration of cardiomyocytes at 6 months (**G**), and 18 months (**K**), though subgross morphology remained normal (**H**, **L**). Original magnification: ×12.5 (**A**, **D**, **E**, **H**, **I**, and **J**); ×400 (**B**, **C**, **F**, **G**, **J**, and **K**). Color-subtractive computer-assisted image analysis and Image J software was used to quantify percentage of collagen in the myocardium (**M**). Levels were not significantly different and both were within the range of normal.

in Figure 5D). This is consistent with the normal electrical conduction seen on the ECGs, and further supported by normal connexin staining on IHC (Supplemental Figure S1, see *http://ajp.amjpathol.org*).

TEM at subsequent ages (8, 10, 12, 14, and 16 months) revealed a persistence of these lesions in A/J mice but not A/HeJ mice, and in addition they had widely scattered individual necrotic cardiomyocytes with myelin figures and vacuolations near the ID (Figure 5F). In the oldest ages (12, 14, and 16 months) there were occasional cardiomyocytes with decreased myofibril density, large accumulations of degenerate mitochondria displacing myofibrils, and collagen in the extracellular matrix (Figure 5G) in both A/J mice and A/HeJ mice.

Aged Dysferlin-Deficient A/J Mice Develop Mild Cardiomyopathy

Since one limitation of TEM is the very small sample size, routine histopathology was used to more broadly assess the progression of changes in the myocardia of A/J mice and A/HeJ mice from 2 to 18 months of age. Initial examination of H&E and Masson's trichrome stained hearts of young (2 to 5 month old) mice revealed that both A/J mice and A/HeJ mice had normal hearts (Figure 6, A and D) and normal cardiomyocytes (Figure 6, B and C). Middle aged (6 month) and aged (18 month) A/HeJ cardiomyocytes were normal (Figure 6, F and J), whereas A/J mice often had widespread sarcoplasmic vacuolar degeneration of cardiomyocytes, often with multiple vacuolations at the ID (Figure 6, G and K). Subgrossly, both A/HeJ and A/J hearts appeared to remain normal (Figure 6, E, H, I, and L).

We then used two methods to more quantitatively assess the development of cardiomyopathy. The development of cardiomyopathy is associated with an increase in interstitial collagen (fibrosis) as the myocardium responds to the loss of cardiomyocytes. Color-subtractive computer-assisted image analysis and Image J software was used to quantify the percentage of collagen in the myocardium (see Methods). This revealed no significant difference in that both A/HeJ and A/J percentages of collagen was about 2% at 2 months of age and gradually increased to about 3% as they aged to 18 months of age (Figure 6M). This suggests little or no cardiomyocyte death in either A/HeJ mice or A/J mice.

Cardiomyopathy is also histopathologically evident as remodeling of the ventricular walls, changes in wall and papillary muscle thickness, degenerative changes that range from vacuolations to necrosis of individual or groups of cardiomyocytes, and changes in nuclear morphology, as well as fibrosis. These more subjective changes can be evaluated for overall significance by an experienced pathologist, so on the same group of sections used for color-subtractive computer-assisted image analysis an experienced pathologist, blinded to the identity of the tissues, scored the sections as normal (0), mild (1), moderate (2), or severe (3) (see Methods). In addition, the thickness of the left ventricular wall was measured with a reticle. As shown (Tables 1 and 2), of the 20 A/HeJ mice examined in this group, 17 (85%) remained normal, one (5%) had mild degenerative changes at 8 months, and two (10%) had mild degenerative changes at 18 months. Left ventricle wall thickness ranged from 1 to 1.6 mm. Of the 22 A/J mice examined, all 4 at 2 months were normal, and 1 of 2 at 6 months was normal; of the 16 A/J mice 8 months or older, only five were normal, the remaining 11 were scored as mild (Table 1). Overall, just under half of the A/J mice were normal, and just over half were scored as mild. None were scored as either moderate or severe. Left ventricle wall thickness ranged from 0.9 to 1.5 mm. These data suggest that the cardiomyopathy of dysferlin null A/J mice under normal laboratory conditions is mild and occurs, when it does, primarily in middle aged to aged mice.

Table 1. Severity of Lesions for A/HeJ Control Mice after H&E and Masson's Trichrome Stained Sections Were Examined Microscopically

Age, mo	Heart Dz	Left ventricular wall, mm
2	0	1.1
2	0	1.2
2	0	1.1
2	0	1.0
6	1	1.0
6	0	1.0
8	0	0.8
8	1	1.5
8	1	1.5
8	1	1.5
10	0	0.9
10	0	0.9
10	1	1.4
12	1	1.4
12	0	1
12	1	1.5
12	1	1
14	1	1
16	1	1
18	1	1
18	1	1.3
18	0	1.3

Severity of lesions present were graded (see *Materials and Methods*) and tabulated under Heart Dz as: 0 = normal; 1 = mild degenerative changes; 2 = moderate degenerative changes; and 3 = severe degenerative changes. The left ventricular wall thickness was measured in millimeters by reticle. Dz, disease.

Discussion

In this study we used the A/J mouse model to investigate the effects of genetically determined dysferlin deficiency by using echocardiography and conscious electrocardiography to determine functional changes *in vivo*, followed postmortem by light and electron microscopy to determine associated morphological changes. We used the A/J mouse model because it is dysferlin null, and therefore a more clear cut model of dysferlin deficiency than the SJL/J mouse that is also dysferlin deficient but still has approximately 15% of the normal levels of dysferlin, thus introducing the complication of low levels of dysferlin.[17] The substrain A/HeJ mice were used as controls since they do not have the A/J dysferlin mutation and so have normal levels of dysferlin and, having a common origin, are the most closely related to the A/J mice. There are only 10 single nucleotide polymorphisms that are different between A/J mice and the substrain A/HeJ. A/HeJ mice have a deletion that renders them unable to secrete complement 5, but this should have no impact on this study. A diligent review of the Mouse Genome Informatics database, JAX Mice database, JAX Genetic Quality Control database, and current literature have revealed no other known genetic differences that would impact this study.

Table 2. Severity of Lesions for Dysferlin-Deficient A/J Mice after H&E and Masson's Trichrome Stained Sections Were Examined Microscopically

Age, mo	Heart Dz	Left ventricular wall, mm
2	0	1
2	0	1.1
2	0	1
6	0	1
6	0	1.1
6	0	1.5
8	0	1.5
8	0	1.5
8	1	1.5
10	0	1
10	0	1.5
12	0	1.3
12	0	1.6
12	0	1
12	0	1
16	0	1
18	0	1.5
18	1	1
18	1	1.1
18	0	1

Severity of lesions present were graded (see *Materials and Methods*) and tabulated under Heart Dz as: 0 = normal; 1 = mild degenerative changes; 2 = moderate degenerative changes; and 3 = severe degenerative changes. The left ventricular wall thickness was measured in millimeters by reticle. Dz, disease.

These results show that in dysferlin-normal mice dysferlin is primarily localized to the ID of the cardiomyocyte and that it is also located in the cardiomyocyte sarcoplasm in a cross-striated pattern with intervals similar to that of Z bands. There are specialized regions of close contact between the sarcoplasmic reticulum and the sarcolemma on either side of the transverse tubules, which are invaginations of the sarcolemma at the Z lines.[18,19] Although protein distribution is not necessarily reflective of protein function, this is a location that contains important membrane proteins in calcium signaling and reuptake, the potential exists for a selective advantage for a membrane repair protein such as dysferlin to be present at this location.[19] Interestingly, there was no evident staining of the lateral sarcolemma. Thus, there appears to be a different pattern of distribution of dysferlin in the cardiomyocyte than in skeletal muscle where it is localized to the lateral sarcolemma. There are different kinds of forces present in the regularly contracting myocardium than in the somewhat temporally unpredictable and varied strength of contractions in skeletal muscle, and the ID is the structure that must maintain tight contact between cardiomyocytes as the force of contraction of adjacent cardiomyocytes acts to pull the ID apart. Membrane damage is inevitable in a kinetically dynamic membranous structure such as the ID and it is reasonable that dysferlin, the primary membrane repair protein of skeletal muscle, should be at this location for the rapid repair of damage to these membranes. If dysferlin is essential for repair, the complete absence of dysferlin, as in dysferlin null A/J mice, should then leave the ID incapable of repair when damage occurs.

Dysferlin-deficient A/J mice developed small vacuolated lesions along the ID as well as in the sarcoplasm away from the ID that were apparent histologically in A/J mice from 6 months of age to 18 months of age. TEM also showed normal ultrastructure at 5 months, but by 6 months there were some membrane delaminations/disruptions and vacuolations in the dysferlin-deficient A/J

mice. Some of these vacuolations were dilations of the sarcoplastic reticulum while others were evident as mitochondria that were swollen to 5 to 10 times normal size with destruction of the cristae (high amplitude swelling). TEM also showed that there were vacuolations not associated with the ID but between myofibrils possibly associated with the transverse tubules as they traverse the sarcomere on either side of the Z disk in close apposition to the sarcoplasmic reticulum (dyads).[19] Similar ultrastructural lesions were present in A/J mice at 8, 10, 12, 14, and 16 months.

The ID is unique to cardiac muscle. Unlike skeletal muscle where one muscle fiber runs the entire length of the muscle, cardiomyocytes are relatively short and connect to neighboring cells from end to end at the ID to form long fibers. The ID has two equally important functions: one is to physically hold the cardiomyocytes tightly together during the forces of contraction; the second is to provide efficient conduction of electrical impulses. Coordinated contraction of the myocardium requires that the depolarization of one cell result in the depolarization of neighboring cells by virtue of current flow through the ID. Disruption of the ID would result in cell-cell uncoupling, ECGs would then show conduction disturbances such as ventricular premature contractions, atrioventricular block, or a widening of QRS duration, due to decreased conduction velocity.[20]

To determine the functional effect of these ID lesions on the electrical conduction of the myocardium, conscious ECGs were performed on A/J and A/HeJ control mice 5 to 20 months of age. It was found that conscious ECGs were not significantly different in any of the durations or amplitudes. These ECGs showed that there were no conduction disturbances associated with these lesions.

These ECGs did, incidentally, show that after 1 year of age heart rates of A/J mice were significantly elevated compared with control A/HeJ mice. This maybe a compensatory mechanism for reduced contractility; however, pain and/or declining cardiovascular conditioning due to the skeletal myopathy of dysferlin deficiency cannot be ruled out as causes.

To answer the question of how the ECGs were normal in the face of the lack of dysferlin at the ID and evidence of vacuolations at this site, tissues were examined by TEM. At the ultrastructural level the ID is a specialized membranous form of the plasma membrane with extensive junctional complexes arranged in transverse plicated areas and longitudinally oriented straighter sections (steps and risers). There are three specialized kinds of junctional complexes of the ID: the fascia adherens; gap junctions; and desmosomes. Desmosomes provide a relatively small but very strong attachment between cells, much like a spot weld. TEM showed there were no abnormalities of the desmosomes in this study.

GJ are distinct membranous substructures of the ID that are regions of low resistance between cells allowing propagation of the action potential from one cell to the next.[21] TEM revealed that in the dysferlin-deficient A/J mice the gap junctions, despite being distorted, appeared to be intact, and the central electron dense area of connexins that lie between membranes display a normal appearance. This would explain the lack of conduction disturbances on ECG examination.

Damage revealed by TEM occurred at the FA. The FA is the site of both the intracellular attachment of the actin cytoskeleton of the contractile elements to the cell membrane as well as attachment to the adjacent cell. This provides efficient transmission of contractile forces but does makes this area vulnerable to contractile stresses.[22,23] The plications of the FA provide a more favorable angle of attachment of tubular elements of the cytoskeleton to the cell membrane and increase the contact area, thus reducing the force per unit area. Failure of the FA of one cardimyocyte to adhere to the FA of the adjacent cardiomyocyte would result in poor force transmission and therefore to poor contractility. If the failure of the FA includes membrane damage this would compromise the integrity of the cardiomyocyte allowing the uncontrolled influx of calcium and lead ultimately to irreversible damage and loss of that cardiomyocyte (for a review see Kumar et al).[24]

To assess overall cardiovascular function, echocardiography was done on these same groups of mice at ages ranging from 5 months to 20 months. Results showed that there was a significant, but temporary, reduction in contractility at 10 months of age. Histopathology at these same intervals showed that morphological changes in the heart remained mild up to 18 months of age. The transient dip in EF and FS could be explained by increased damage from cardiovascular loads associated with activity as these mice grew older and heavier followed by decreasing cardiovascular loads as the skeletal muscles degenerate to the point that these mice no longer tax the cardiovascular system. The debilitating effects of severe skeletal muscle degeneration would thus be providing some protection to the heart against continuation of the decline in EF and FS. If this were the only change, one would expect that there would not be further deterioration of EF and FS, but the improved EF and FS in these older A/J mice suggests that there are dysferlin-independent means of repairing damaged membranes before the onset of irreversible cellular damage.

It is noteworthy that our results were obtained from unmanipulated mice living under sedentary laboratory conditions. In 2007, two independent studies[8,11] showed that with the introduction of elevated cardiac stress, the EF and FS were significantly reduced. In one of these studies[11] it was noted that 40% of A/J mice did not survive beyond 3 days of a standardized regimen of pharmacologically increased cardiac stress, although no data on cause of death was shown. The observation that these A/J mice died in 3 days combined with our finding that 1½-year-old A/J mice develop only mild cardiomyopathy suggests that more damage occurred in 3 days as a result of moderately increased loads than occurs in 1½ years under ordinary husbandry conditions.

We know that damage to the plasma membrane is not being avoided based on the persistence of vacuolations in many A/J mice from 6 months of age to 18 months of age, and Han et al[8] showed that troponin levels are chronically elevated, yet older animals have nearly normal myocardia. This could be explained by the presence

of a second repair mechanism that is activated only when the dysferlin mechanism fails but is slower and cannot protect against sudden widespread damage. Another possible explanation is that, in cardiac muscle, dysferlin plays a role in the final attachment of, or the intrinsic strength of, the membrane repair patch. If this were the case, in dysferlin-deficient cardiomyocytes the membrane disruption may be sealed, but with a patch that is weak, or attached weakly, but just strong enough to restore the integrity of the cardiomyocyte in moderate conditions. A relatively small increase in cardiac stress could then cause a global failure of pre-existing repairs.

The presence of the vacuolated areas adjacent to the ID may be an adaptive "make-shift" repair or may represent another, slower, cardiac specific dysferlin-independent repair mechanism that restores the integrity of the plasma membrane to prevent irreversible injury to the cardiomyocyte but is not resilient enough to withstand elevated cardiac stress.

These data suggest that without dysferlin, cardiac muscle cells, like skeletal muscle cells, may perform normally for a period of time but then sustain small membrane defects that are not repaired normally. This damage occurs at a younger age in skeletal muscle than cardiac muscle perhaps due to differences in the rate at which cardiac membranes are damaged, or to the possibility that there are other factors/repair mechanisms that provide cardiac muscle with a more robust, or functionally redundant, membrane repair system than skeletal muscle. The presence of demonstrable membrane damage in 6-month-old dysferlin-deficient mice and persistence of vacuoles at older ages is evidence that it is not merely increased resilience that reduces the incidence of irreversible cell damage in the cardiomyocyte.

In summary, this study has shown that dysferlin is localized primarily to the ID of the cardiomyocyte, and to a lesser extent in a cross-sarcomeric pattern in the sarcoplasm. Light and electron microscopy show lesions at these locations in dysferlin-null A/J mice that are consistent with defective membrane repair. Echocardiography shows a transient decrease in cardiac function at around 10 months of age yet aged unmanipulated dysferlin-deficient mice progress only to mild cardiomyopathy. The data in this study suggest that in cardiac muscle of dysferlin-null A/J mice membrane damage is occurring, injury to the cardiomyocyte is evident, the repair mechanism maybe defective and delayed, but the damage is resolved before leading to the demise of the cardiomyocyte.

Future studies will focus on extending the search for additional mechanisms by which cardiac muscle restores membrane integrity without dysferlin under normal and stressed conditions. More complete knowledge of the means by which dysferlin-deficient mice limit cardiomyocyte damage or employ other, perhaps slower, pathways to repair or prevent membrane damage may lead to therapeutic targets or genetic interventions that could be transferable to skeletal muscle to ameliorate the severity of skeletal muscle disease in dysferlin-deficient patients.

Acknowledgments

We thank Anthony Nicholson, PhD, BVSc, and Jennifer L. Ryan for expert technical help with the ECG and echocardiography. We are grateful to Ed Leiter and Roger Sher for their valuable comments.

References

1. Clarke MS, Caldwell RW, Chiao H, Miyake K, McNeil PL: Contraction-induced cell wounding and release of fibroblast growth factor in heart. Circ Res 1995, 76:927–934
2. Miyake K, McNeil PL: Mechanical injury and repair of cells. Crit Care Med 2003, 31:S496–S501
3. Bansal D, Miyake K, Vogel SS, Groh S, Chen CC, Williamson R, McNeil PL, Campbell KP: Defective membrane repair in dysferlin-deficient muscular dystrophy. Nature 2003, 423:168–172
4. Liu J, Aoki M: Dysferlin, a novel skeletal muscle gene, is mutated in Miyoshi Myopathy and limb girdle muscular dystrophy 2B. Nat Genet 1998, 20:31–36
5. Bashir R, Britton S, Strachan T, Keers S, Vafiadaki E, Lako M, Richard I, Marchand S, Bourg N, Argov Z, Sadeh M, Mahjneh I, Marconi G, Passos-Bueno MR, Moreira Ede S, Zatz M, Beckmann JS, Bushby K: A gene related to Caenorhabditis elegans spermatogenesis factor fer-1 is mutated in limb-girdle muscular dystrophy type 2B. Nat Genet 1998, 20:37–42
6. Anderson LV, Davison K, Moss JA, Young C, Cullen MJ, Walsh J, Johnson MA, Bashir R, Britton S, Keers S, Argov Z, Mahjneh I, Fougerousse F, Beckmann JS, Bushby KM: Dysferlin is a plasma membrane protein and is expressed early in human development. Hum Mol Genet 1999, 8:855–861
7. Matsuda C, Aoki M, Hayashi YK, Ho MF, Arahata K, Brown RH, Jr: Dysferlin is a surface membrane-associated protein that is absent in Miyoshi myopathy. Neurology 1999, 53:1119–1122
8. Han R, Bansal D, Miyake K, Muniz VP, Weiss RM, McNeil PL, Campbell KP: Dysferlin-mediated membrane repair protects the heart from stress-induced left ventricular injury. J Clin Invest 2007, 117:1805–1813
9. Lennon NJ, Kho A, Bacskai BJ, Perlmutter SL, Hyman BT, Brown RH, Jr: Dysferlin interacts with annexins A1 and A2 and mediates sarcolemmal wound-healing. J Biol Chem 2003, 278:50466–50473
10. Kuru S, Yasuma F, Wakayama T, Kimura S, Konagaya M, Aoki M, Tanabe M, Takahashi T: A patient with limb girdle muscular dystrophy type 2B (LGMD2B) manifesting cardiomyopathy. Rinsho Shinkeigaku 2004, 44:375–378
11. Wenzel K, Geier C, Qadri F, Hubner N, Schulz H, Erdmann B, Gross V, Bauer D, Dechend R, Dietz R, Osterziel KJ, Spuler S, Ozcelik C: Dysfunction of dysferlin-deficient hearts. J Mol Med 2007, 85:1203–1214
12. Ho M, Post CM, Donahue LR, Lidov HG, Bronson RT, Goolsby H, Watkins SC, Cox GA, Brown RH, Jr: Disruption of muscle membrane and phenotype divergence in two novel mouse models of dysferlin deficiency. Hum Mol Genet 2004, 13:1999–2010
13. Vasiljevic JD, Popovic ZB, Otasevic P, Popovic ZV, Vidakovic R, Miric M, Neskovic AN: Myocardial fibrosis assessment by semiquantitative, point-counting and computer-based methods in patients with heart disease: a comparative study. Histopathology 2001, 38:338–343
14. Gaspard GJ, Pasumarthi KB: Quantification of cardiac fibrosis by colour-subtractive computer-assisted image analysis. Clin Exp Pharmacol Physiol 2008, 35:679–686
15. Maddatu TP, Garvey SM, Schroeder DG, Hampton TG, Cox GA: Transgenic rescue of neurogenic atrophy in the nmd mouse reveals a role for Ighmbp2 in dilated cardiomyopathy. Hum Mol Genet 2004, 13:1105–1115
16. Sutton P: Measurements in Cardiology. 1999
17. Bittner RE, Anderson LV, Burkhardt E, Bashir R, Vafiadaki E, Ivanova S, Raffelsberger T, Maerk I, Hoger H, Jung M, Karbasiyan M, Storch M, Lassmann H, Moss JA, Davison K, Harrison R, Bushby KM, Reis A: Dysferlin deletion in SJL mice (SJL-Dysf) defines a natural model for limb girdle muscular dystrophy 2B. Nat Genet 1999, 23:141–142
18. Challice C, Viragh S: Ultrastructure of the Mammalian Heart. New York, Academic Press, 1973, pp 19–23

19. Brette F, Orchard C: Resurgence of cardiac t-tubule research. Physiology 2007, 22:167–173
20. Cheng CF, Kuo HC, Chien KR: Genetic modifiers of cardiac arrhythmias. Trends Mol Med 2003, 9:59–66
21. Rucker-Martin C, Milliez P, Tan S, Decrouy X, Recouvreur M, Vranckx R, Delcayre C, Renaud JF, Dunia I, Segretain D, Hatem SN: Chronic hemodynamic overload of the atria is an important factor for gap junction remodeling in human and rat hearts. Cardiovasc Res 2006, 72:69–79
22. Basso C, Czarnowska E, Della Barbera M, Bauce B, Beffagna G, Wlodarska EK, Pilichou K, Ramondo A, Lorenzon A, Wozniek O, Corrado D, Daliento L, Danieli GA, Valente M, Nava A, Thiene G, Rampazzo A: Ultrastructural evidence of intercalated disc remodelling in arrhythmogenic right ventricular cardiomyopathy: an electron microscopy investigation on endomyocardial biopsies. Eur Heart J 2006, 27:1847–1854
23. Sheikh F, Chen Y, Liang X, Hirschy A, Stenbit AE, Gu Y, Dalton ND, Yajima T, Lu Y, Knowlton KU, Peterson KL, Perriard JC, Chen J: Alpha-E-catenin inactivation disrupts the cardiomyocyte adherens junction, resulting in cardiomyopathy and susceptibility to wall rupture. Circulation 2006, 114:1046–1055
24. Kumar V, Abbas A, Fausto N: Pathologic Basis of Disease. Philadelphia, Elsevier Saunders, 2005, pp 14–34